Electric power conversion of exhaust waste heat recovery from gas turbine power plant using organic Rankine cycle

S. O. Oyedepo & A. B. Fakeye

International Journal of Energy and Water Resources

ISSN 2538-3604

Int J Energ Water Res
DOI 10.1007/s42108-019-00055-3

ONLINE FIRST

Springer

International Journal of Energy and Water Resources
https://doi.org/10.1007/s42108-019-00055-3

ORIGINAL ARTICLE

Electric power conversion of exhaust waste heat recovery from gas turbine power plant using organic Rankine cycle

S. O. Oyedepo[1] · A. B. Fakeye[1]

Received: 28 November 2018 / Accepted: 26 December 2019

Abstract

In this study, an examination of a bottoming organic Rankine cycle for power conversion of the flue gases from a 5.75 MW gas turbine power plant was carried out. First law of thermodynamics was applied to the four major components of the system and simulated using developed MATLAB codes, while the thermo-physical properties at each state were supplied by engineering equation solver database. Five organic working fluids were compared based on selected performance indices. Toluene exhibited the best performance at full and partial electric generator load conditions with net power outputs of 532.70 kW at full load and 412.95 kW at partial load of 75%, while at 50% partial load, R245fa has the highest net power output of 469.09 kW. The cycle efficiency of the organic Rankine cycle system was improved from 34.67% at full load to 40.51% with exhaust gases from the power plant considered as sources of low-grade heat. R245fa showed the best adaptability at 50% partial load but at excessively high mass flow rate of 13.62 kg/s. It is evidently shown from this study that, waste heat recovery technologies can effectively generate about 16.8% of the nominal power of a gas turbine power plant and hence, reduce emissions per kW generated, suitable for sustainable environment as well as promoting energy security.

Keywords Power cycle · Thermal efficiency · Organic working fluids · Performance indices · Recuperator · Heat recovery unit

Abbreviations

h	Enthalpy
i	Ideal
$\dot{m}$	Mass flow rate
P	Pressure
Q	Heat flow
s	Entropy
T	Temperature
W	Mechanical power
1, 2, 2′, 3″, 3, 4, 5	Thermodynamic states
a	Actual state
b	Boiler
c	Condenser
des	Desuperheater
ev	Evaporator
g	Exhaust gas
GT	Gas turbine
I	Isentropic
p	Pump
pr	Preheater
r	Real state
ref	Refrigerant (working fluid)
rej	Rejected
s	Isentropic state
sp	Superheater
w	Unit power, power output
ref	Refrigerant (working fluid)
BWR	Back work ratio
DSH	Degree of superheating
EES	Engineering equation solver
EGL	Electric generator load
HRU	Heat recovery unit
LHV	Lower heating value of fuel
ORC	Organic Rankine cycle
WHR	Waste heat recovery

Electronic supplementary material The online version of this article (https://doi.org/10.1007/s42108-019-00055-3) contains supplementary material, which is available to authorized users.

✉ S. O. Oyedepo
sunday.oyedepo@covenantuniversity.edu.ng

[1] Mechanical Engineering Department, Covenant University, Ota, Nigeria

Published online: 10 February 2020

Introduction

Typically, low conversion efficiencies of gas turbine power plants indicates the unsustainable pattern of energy utilization. This inherently means that as much huge amount of low-grade waste heat resource is daily wastefully lost in various heat streams, while at the same time depositing excessive and avoidable amount of toxic emissions into the environment. This in essence leads to over-exploitation of the limited resources and also causing excessive degradation of the environment. This has, therefore, attracted global attention to make the utilization of the resource conform to the goals of sustainable development. Recovery and reuse of the degraded heat from such thermal processes and systems is generally a sustainable way of fossil fuel consumption as it offers significant potential for substantial reduction in global fuel consumption and carbon footprint (Xiaojun et al. 2016).

Organic Rankine cycles (ORCs) are widely proposed for waste heat-to-power conversion of exhaust gases, because they are characteristically simple-structured, reliable, easy to maintain, modify and adapt to various heat sources (Bao and Zhao 2013; Feng et al. 2015) and may be operated in subcritical or transcritical cycles. The ORC is a heat-to-power conversion technology that has been in use since 19th century making use of low-grade temperature sources between 80 and 300 °C but the temperature range is now widening due to development of new applications (Landelle et al. 2017; Xiao et al. 2015). The ORC with a regenerative heat exchanger can reduce the heat input to the system and improve the thermal efficiency by preheating the working fluid entering the evaporator, and the cascaded ORC can achieve an improved performance. Combined cycles based on ORC also can utilize the energy source more efficiently. Various cycles, such as the combined cycle of an ORC and refrigeration; combined cycle of ORC and liquefied natural gas (LNG) cold energy; combined cooling, heating, and power generation cycle; and solar ORC have been proposed and investigated (Abadi and Kim, 2017). Waste heat sources available for recovery from various heat sources are capable of effectively powering ORC systems to deliver output energy scales ranging from about 10 kW to 10 MW (Auld et al. 2013).

Various works have been done on the feasibility of ORC systems design. Diverse configurations with various performance indices have been investigated. Safarian and Aramoun (2015) exploited energy and exergy optimization of a basic and three modified ORCs, i.e., ORC integrated with turbine bleeding, regenerative ORC, and an ORC incorporating both turbine bleeding and regeneration, to study the influence and effectiveness of such modifications on the performance of ORC. The basic ORC showed the lowest exergy efficiency and also the highest exergy losses, while the modified ORCs showed improved evaporator exergy losses by 5.5%, 48.5%, and 55%, respectively, as mentioned. Turbine bleeding reduces the gross power output of the cycle but the combined effect of the optimized turbine bleeding with the corresponding improved exergy losses cannot be concluded to effectively improve the net power output of an ORC cycle for waste heat recovery based on available literature (Wenqiang et al. 2017).

The exergy analysis which is an analysis of energy conversion systems based on the Second law of thermodynamic. This analysis gives a clearer description of the system performance and its losses (Chen 2011). In optimization of ORC system using exergy analysis, the exergetic efficiency criteria are unaffected by the heat source temperature (Wang et al. 2015) hence, it is insufficient to optimize ORC system by not factoring the adaptability of the ORC to the specific operating condition under consideration. Significant parameters for exergy efficiency and cost implication include turbine inlet pressure and temperature, pinch temperature difference, approach temperature difference and condenser temperature difference (Xiao et al. 2015; Li et al. 2019). Researches have severally established that maximizing power output rather than the thermal or exergetic efficiency is critical to waste heat recovery (Donghong et al. 2007; Pierobon et al. 2013; Tailu et al. 2015; Roberto and Lars, 2017).

Hence, Kai et al. (2015) investigated the effect of evaporation pressure, degree of superheat, and the minimum allowable temperature in the evaporator of an ORC geothermal application. Results indicated that the effect of pinch temperature in the evaporator on the unit power is much more significant than that of superheating. However, Badescu et al. (2017) established that an optimum evaporation pressure exists for which the net power attains the maximum, both of which are a function of degree of superheat when utilizing isentropic fluids and that dry fluids require no superheating. The optimum degree of superheat was said to range between 30 and 40 °C for isentropic working fluids depending on the type of at both full and partial loads design conditions. It has likewise been established that the use of a recuperator or regeneration with turbine bleeding, however, reduces the amount of heat that can be transferred to the cycle from the waste heat source (Abadi and Kim, 2017).

Nonetheless, the recuperator contributes more than improving the cycle efficiency, it also retains the minimum fluid temperature required by the heat recovery vapor generator to prevent corrosion as a result of condensation of sulfur components in the exhaust gases (Hattiangadi, 2013), as well as significantly decreasing the condenser load (Guo et al. 2015). Hence, it is of benefit to consider the optimal amount of superheat as well as recuperation for detailed design analysis when using isentropic fluids (Dubberke et al. 2018). The use of recuperator is, however, more essential when using dry fluids as dry working fluid is still superheated at the exit of the turbine and may hence be used to preheat the fluid going into the evaporator, hence reducing the temperature of the fluid to the condensing temperature corresponding to the two-phase state (Rusev, 2014; Yu et al. 2016).

Table 1 presents brief summary of various works on feasibility of organic Rankine cycle in conversion of low-grade heat to electricity.

The basic ORC, therefore, has been identified as the best cycle design configuration in both economic and thermodynamic perspective for preliminary design stage, especially for waste heat recovery applications (Lecompte et al. 2015). Likewise, Li et al. (2012) attested that internal heat exchanger (IHE) cannot increase the net power output at a given heat source condition and also agreed that the superheating and supercooling of the working fluids invariably lead to an increase in the system irreversibilities and hence considered the basic ORC system ideal for a similar study.

The aim of this study is to carry out a technical feasibility of waste heat-to-power conversion of the exhaust of a 5.77 MW gas turbine power plant using organic Rankine cycle (ORC). A thermodynamic model for a suitable ORC architecture was developed to study the feasibility of the power conversion. The model was executed in MATLAB codes, while the thermodynamic data for the selected working fluids were furnished by EES database. Comparisons of the performances of the organic fluids are hence made at similar operating conditions subject to a set of constraints. This study was carried out in May 2018 at Covenant University, Ota, Nigeria.

Materials and methods

The ORC system design data are presented in Table 2. The governing equations are developed in this section and the maximum net power output computed using the developed MATLAB codes linked with EES to supply the thermodynamic properties of the pre-selected working fluids at each state. The system layout of the basic ORC adopted for the feasibility assessment (Li et al. 2012) of the selected 5.67 MW Solar Taurus gas turbine powering Covenant University located Canaan land, Ota, Nigeria is schematically depicted in Fig. 1, while Fig. 2 shows the typical temperature profile for the adopted ORC unit.

Formulation of governing equations

As depicted in Fig. 1, the main components consist of a condenser, the working fluid pump, heat recovery unit, and the expander. The heat recovery unit (HRU), commonly referred to as evaporator, conceptually consists of three

Table 2 ORC system design data

Pump efficiency (%)	80
Turbine inlet Temperature, TIT (K)	100–350
Turbine efficiency (%)	87
Turbine inlet pressure TIP (bar)	15–30
Heat exchangers effectiveness	0.95

Table 1 Summary on feasibility study of ORC system design

S/N	Author(s)	Work	Findings/remarks
1	Guo et al. (2015)	Investigated power recovery from exhaust gases using pure and zeotropic fluids for ORC applying a number of performance indicators	There is no optimal working fluid that can satisfy all the performance indices at once. Power developed and investment consideration are most important. R600a, R601
2	Xi et al. (2015)	Effect of zeotropic mixtures on ORC for WHR	Zeotropic mixtures increases work output but heat transfer area and equipment cost increases considerably
3	Rusev (2014)	WHR from combined cycle system of solid oxide fuel cell and gas turbine with ORC bottoming cycle from first law of thermodynamics	System efficiency increased by 8–12%. R141b, R254fa, R236fa
4	Cao et al. (2016)	Optimum design for recuperative ORC for WHR from gas turbine	Net power and thermal efficiency of recuperative ORC increases with rise in the ORC turbine inlet pressure. Toluene is the most suitable for fluid with optimum pressure of 3.35 Mpa
5	Eveloy et al. (2016)	Thermodynamic analysis of WHR from gas turbine using ORC	22.3% extra power could be generated from a 22.2 MW base load industrial gas turbine power plant using R245fa
6	Carcasci et al. (2014)	Thermodynamic analysis of WHR from gas turbine using ORC using thermal loop	Superheating in not essential for toluene, benzene and cyclohexane but their suitability depends on the temperature of the thermal loop oil. Cyclopentane require superheating and as well showed worst performance. Toluene is best at high oil temperature

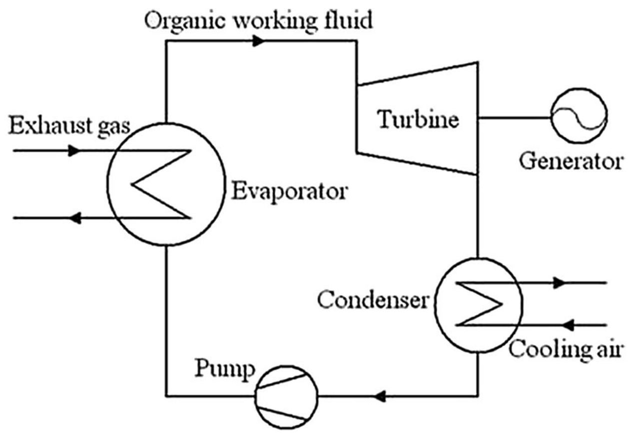

Fig. 1 Schematic of basic ORC

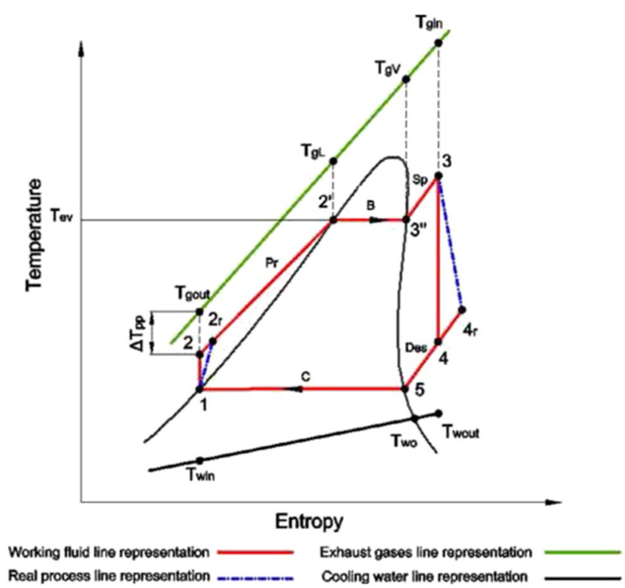

Fig. 2 Typical temperature profile for adapted ORC configuration

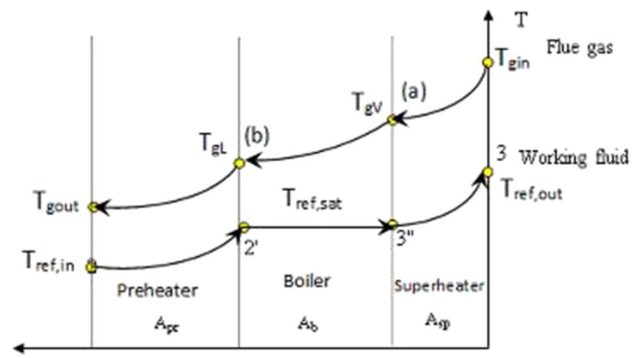

Fig. 3 The three zones of HRVG (preheater, boiler and superheater)

sections namely preheater or economizer (section 1), boiler or evaporator (section 2), and the superheater (section 3) which are connected in series with a fixed total area but variable section areas for the three sections depending on the operating regime (Fig. 3). For dry and isentropic fluids, the condenser essentially consists of two sections namely the desuperheater and the condensation sections.

Properties of the flue gas

The type of fuel used in combustion process determines the composition of the exhaust gases. The main components in the flue gas resulting from combustion of fossil fuels driving electric generators are CO_2, H_2O, N_2, and O_2. The gas turbine power plant in consideration can be alternatively fired by diesel. A typical composition of combustion products generated from natural gas combustion as given by Sung et al. (2016) are 72.55% nitrogen, 12.34% oxygen, 3.72% carbon dioxide, 10.52% water and 0.87% argon, while that adopted by Badescu et al. (2017) for combusting diesel fuel is 9.1% carbon dioxide, 7.4% water, 9.3% oxygen and 74.2% nitrogen. However, the mass fractions of these constituents vary depending on operating regime subject to whether it bears full or partial load. Since the power plant is mostly fired by natural gas, the mass fraction by Sung et al. (2016) is adopted for estimating flue gas properties.

Assuming steady state of the system, the enthalpy of the mixture of the exhaust gases can be obtained as the weighted sum of each constituent of the mixture (Reis and Gallo, 2018), expressed as

$$h_{\mathrm{gmix}} = \sum_{n=1}^{5} mf_n \cdot h_n, \tag{1}$$

where mf_n is the mass fraction in % of the each of the five constituents.

Thermodynamic model of ORC components

This section presents the thermodynamic model of the basic equations and technical analysis for each of the four main components of ORC in sequence of flow/process.

Assumptions and constraints

To simplify the thermodynamic model of the ORC, the following assumptions are made:

In this study, it is considered that:

- The system operates in a steady-state condition; kinetic and potential energy changes are neglected.
- Pressure drops in pipelines are neglected.

- The saturation pressure at ambient temperature had to be higher than 1 kPa to limit vacuum in the condenser.
- The system's components of the cycle are thermally insulated.
- The working fluid condensing pressure has been imposed to be higher than 1.2 bar to avoid ambient air leaking into the system and expensive sealing;
- Minimum pinch point temperature difference (Δ_{pp}) between $_{\text{gout}}$ and $_{2} = 10$ °C, hence, $_{2} \geq 80$ °C to maintain the exit temperature of the exhaust gas at minimum of 90 °C.
- Stepwise increase in degree of superheat = + 2 °C.
- Expander isentropic efficiency $\eta_{\text{exp}} = 0.87$.
- Pump isentropic efficiency $\eta_{\text{pump}} = 0.80$.
- Heat exchangers effectiveness is approximately 0.95.

Model of pump

The working fluid from the condenser at saturated liquid state 1 flows into the pump where it undergoes an ideal isentropic process from the state 1 to state 2, but actually to state 2*r* at the exit of the pump because of irreversibilities (Fig. 2). The work input added by the pump to the working fluid and the unit work added are thus expressed as

$$W_{\text{P.actual}} = \frac{\dot{w}_{\text{pact}}}{\eta_{\text{P}}} = \frac{\dot{m}_{\text{ref}}\left(h_1 - h_{2r}\right)}{\eta_{\text{P}}} = \dot{m}_{\text{ref}}\left(h_1 - h_{2r}\right), \tag{2}$$

$$W_{\text{P.ideal}} = \frac{\dot{w}_{\text{p,ideal}}}{\eta_P} = \frac{\left(h_1 - h_2\right)}{\eta_P} = \dot{m}_{\text{ref}}\left(h_1 - h_2\right), \tag{3}$$

where $W_{\text{P.actual}}$ is the actual power consumed by the pump, $W_{\text{p,ideal}}$ is the ideal power consumed by the pump, $\dot{w}_{\text{pact}}$ and $\dot{w}_{\text{pideal}}$ are rates of actual and ideal pump works, respectively, $\dot{m}_{\text{ref}}$ is the mass flow rate of the organic working fluid, η_{P} is the pump isentropic efficiency, h_1 is the working fluid enthalpy at the pump inlet, and h_2 and h_{2r} are the isentropic and actual enthalpies of the working fluid at the pump outlet, respectively, for the ideal case.

Two intensive properties are required to define the state of the fluid at any point. The enthalpy at state 1 (h_1) can be determined as a function of the temperature and pressure. The pressure, however, depends not only on temperature but on the vapor quality as well. Since the liquid is saturated at state 1, the pressure hence depends solely on the temperature. Other properties such as the specific enthalpy, entropy, etc. at state 1 can be determined at the saturated liquid values.

Since process 1–2 is isentropic, meaning that the entropies at states 1 and 2 are ideally the same, it is, therefore, required to know one other property to obtain other properties at state 2. Initially, an estimate of the evaporation pressure is made close to, but lower than, the critical pressure of the pre-selected working fluid to evaluate other essential properties at state 2 such as the temperature and the specific enthalpy. To account for errors associated with assumptions and also to keep the design within practically achievable limits, pressure boundary conditions adopted are $0.01P_{\text{crit}} < P < 0.81P_{\text{crit}}$ (Auld et al. 2013; Quoilin et al. 2011). However, for safety consideration and possible chemical instability of the organic fluids, the maximum allowable cycle pressure is limited to 30 bar (Quoilin et al. 2011).

Model of heat recovery unit (HRU)

Since processes 2–3″ are constant pressure heat addition processes in the HRU, hence, $P_{\text{ev}} = P_{2r} = P_3 = P_{3''}$. The specific enthalpy of state 2*r* can, therefore, be evaluated as a function of pump efficiency (assumed constant) as

$$h_{2r} = h_1 + \frac{\left(h_2 - h_1\right)}{\eta_P}. \tag{4}$$

Hence, the evaporation temperature T_{ev} is equivalent to the saturation temperature of the working fluid corresponding to the evaporation pressure at state 2*r*. The values of the specific enthalpy can hence be obtained. Consequently, the inlet expander temperature at state 3″ can then be generated from

$$T_3 = T_{\text{ev}} + \Delta T_{\text{sp}}, \tag{5}$$

where ΔT_{sp} is the stepwise superheating increment over the evaporation temperature. As the two compulsory thermodynamic properties (temperature and pressure) at the turbine inlet are known thus, the enthalpy at the superheated state 3 can be determined.

The process between states 3 and 4 is ideally an isentropic process, thus, the entropies at states 3 and 4 are equal ($s_3 = s_4$). In addition, the pressure at state 1 is the same as condensation pressure at state 4 ($P_1 = P_4$). Hence, the other parameters at state 4—the temperature and the specific enthalpy can likewise be determined. The specific enthalpy h_{4r} at state 4*r* can hence be evaluated based on the expander efficiency from

$$h_{4r} = h_3 + \frac{\left(h_3 - h_4\right)}{\eta_{\text{exp}}}. \tag{6}$$

So far, all the required information about the entire processes taking place in the ORC has thus been obtained, whereas, only the temperature of the exhaust gas which is the heat source temperature to the evaporator is not hitherto known, except the inlet flue gas temperature to the evaporator, which averages between the range of 363 °C at 50% load to 520 °C at full load as shown in Table 3 [as obtained from

Table 3 Operating parameters of the gas turbine at full and partial loads

S/N	Operating parameters	Values
1	Exhaust gas temperature@100%	510 °C
2	Exhaust mass flow rate@100%	21.77 kg/s
3	Exhaust gas temperature@75%	450 °C
4	Exhaust mass flow rate@100%	19.89 kg/s
5	Exhaust gas temperature@50%	366 °C
6	Exhaust mass flow rate@50%	18.64 kg/s

Efficiency Department of Canaan land Independent Power Project (CIPP)]. It is appropriate to start up the ORC design with the assumption of full load where the flue gas temperature is 510 °C and the flue gas mass flow rate is 21.774 kg/s. Subsequently, 75% load and 50% load are thereafter considered.

A minimum pinch point temperature difference (ΔT_{pp}) between T_{gout} and T_2 of 10 °C is considered as a trade-off between meeting the gas heat exchanger performance and the cost-dimension factor (Quoilin et al. 2011). The minimum pinch point temperature difference is adapted to maintain the temperature of the flue gas at the outlet of the HRU to be 90 °C at minimum as prescribed for waste heat recovery applications to avoid condensation of toxic gases in the exhaust (Sung et al. 2016; Zhou et al. 2013). The heat transfer from the flue gas to the working fluid may be treated in two steps as recommended by Badescu et al. (2017):

Step 1: Restricting the pinch point to the heat source outlet allows the maximum energy absorption from the waste heat in the HRU. The minimum pinch point temperature difference ΔT_{pp} is, therefore, assumed to occur between state 2 and T_{gout}, which implies $T_{gout}=T_2+\Delta T_{pp}$, hence the minimum temperature T_2 that can be attained is 80 °C. Then, the energy balance associated with full evaporation and superheating of the working fluid may be given as

$$\dot{m}_{ref}\left(h_3 - h_2\right) = \dot{m}_g C_{Pg1}\left(T_{gin} - T_{gout}\right). \tag{7}$$

Then

$$\dot{m}_{ref} = \frac{\dot{m}_g C_{Pg1}\left(T_{gin} - T_{gout}\right)}{\left(h_3 - h_2\right)}, \tag{8}$$

where the specific heat capacity C_{Pg1} is evaluated based on the flue gas composition at the average temperature between T_{gout} and T_{gin} (as the different between T_1 and T_2 is not significantly high).

Step 2: To evaluate the temperatures of the exhaust gas at the boiler inlet (T_{gL}) and the superheater inlet (T_{gV}), two other energy equations involving the parameters are

$$\dot{m}_{ref}\left(h_{2'} - h_2\right) = \dot{m}_g C_{Pg2}\left(T_{gL} - T_{gout}\right). \tag{9}$$

$$\dot{m}_{ref}\left(h_{3''} - h_{2'}\right) = \dot{m}_g C_{Pg3}\left(T_{gV} - T_{gL}\right). \tag{10}$$

The temperatures of the exhaust gas at boiler inlet and superheater inlet are, respectively, given as

$$T_{gL} = T_{gout} + \frac{\dot{m}_{ref}\left(h_{2'} - h_2\right)}{\dot{m}_g C_{Pg2}}. \tag{11}$$

$$T_{gV} = T_{gL} + \frac{\dot{m}_{ref}\left(h_{3''} - h_{2'}\right)}{\dot{m}_g C_{Pg3}}. \tag{12}$$

The specific heat capacities C_{Pg2} and C_{Pg3} are, respectively, evaluated at the average temperature between T_{gout} and T_{gL}, and between T_{gL} and T_{gV}.

Hence, as shown in Figs. 2 and 3, four temperature differences are obtainable between the exhaust gas and the working fluid during the working fluid heat addition process 2–3 which are: $\Delta T_{in}=T_{gin} - T_3$, $\Delta T_V=T_{gV} - T_{eV}$, $\Delta T_L = T_{gL} - T_{eV}$, and $\Delta T_{out}=T_{gout} - T_2$, respectively. $\Delta\ T_{out}$ is expected to be the smallest temperature difference among the four temperature differences and, therefore, is taken as the pinch point temperature difference.

Model of expander

The work extracted from the working fluid is converted into shaft work in expander. The power developed by the expander is given by

$$W_{exp,actual} = \eta_{exp}.W_{exp,ideal} = \eta_{exp}.\dot{m}_{ref}\left(h_3 - h_4\right) = \dot{m}_{ref}\left(h_3 - h_{4r}\right) \tag{13}$$

where $W_{exp,ideal}$ is the ideal power developed by the expander, η_{exp} is the isentropic efficiency of the expander, and h_3 and h_{4r} are, respectively, the actual specific enthalpies of the working fluid at the expander inlet and outlet.

Model of condenser

The heat rejected in the condenser (both for desuperheating and condensation) can thus be determined using Eq. (14):

$$Q_{rej} = \dot{m}_{ref}\left(h_{4r} - h_1\right). \tag{14}$$

As also shown in Fig. 2, there are three temperature differences between the working fluid and the cooling water during the cooling processes 4–1: $\Delta T_{c.in}=T_1 - T_{win}$, $\Delta T_{c.m}=T_5 - T_{wo}$, and $\Delta T_{cout}=T_4 - T_{wout}$, correspondingly. To prevent inverse heat transfer under extremely hot ambient conditions, condensing and evaporating temperatures must, however, be higher than 50 °C and the minimum condensing pressure is 1.2 bar so as to prevent ambient air leaking into the system and at the same time, avoid expensive sealing (Zhou et al. 2013).

Heat fluxes for heat recovery unit

The total heat flux, heat flux in the superheater, boiler and the preheater can, respectively, be expressed as

$$Q_{\text{source}} = \dot{m}_{\text{ref}}\left(h_3 - h_2\right). \tag{15}$$

$$Q_{\text{sp}} = \dot{m}_{\text{ref}}\left(h_3 - h_{3''}\right). \tag{16}$$

$$Q_{\text{b}} = \dot{m}_{\text{ref}}\left(h_{3''} - h_{2'}\right). \tag{17}$$

$$Q_{\text{pr}} = \dot{m}_{\text{ref}}\left(h_{2'} - h_2\right). \tag{18}$$

As well, addition of heat fluxes for the three sections is equal to the total heat flux for the HRU:

$$Q_{\text{source}} = Q_{\text{sp}} + Q_{\text{b}} + Q_{\text{pr}}. \tag{19}$$

Heat fluxes for condenser

As well, the heat total rejection in the condenser and the heat rejected during desuperheating and condensation can be expressed as

$$Q_{\text{rej}} = \dot{m}_w C_w \left(T_{\text{wout}} - T_{\text{win}}\right). \tag{20}$$

$$Q_{\text{des}} = \dot{m}_{\text{ref}}\left(h_{4r} - h_5\right). \tag{21}$$

$$Q_{\text{condensation}} = \dot{m}_{\text{ref}}\left(h_5 - h_1\right). \tag{22}$$

However

$$Q_{\text{rej}} = Q_{\text{des}} + Q_{\text{condensation}}. \tag{23}$$

Performance indices of ORC unit

Four indices selected for evaluating the performance of the ORC unit are given below.

Heat recovery efficiency

An efficiency indicator for the heat recovery process that takes place in the HRU as cited to be proposed by Zhou et al. (2013) and employed by Hattiangadi (2013) is the heat recovery efficiency. The heat recovery efficiency η_{r} is defined as the fraction of the heat flux absorbed by the working fluid from the exhaust gas to the maximum heat flux Q_{max} which can be recovered from the flue gas:

$$\eta_r = \frac{Q_{\text{gases}}}{Q_{\text{max}}} = \frac{\dot{m}_{\text{ref}}\left(h_3 - h_2\right)}{\dot{m}_{\text{g}} C_{\text{P,g}}\left[T_{\text{gin}} - \left(T_2 + \dot{m}T_{\text{amb}}\right)\right]}, \tag{24}$$

where Q_{max} is given by

$$Q_{\text{max}} = \dot{m}_{\text{g}} C_{\text{P,g}}\left[T_{\text{gin}} - \left(T_2 + \Delta T_{\text{amb}}\right)\right], \tag{25}$$

$\dot{m}_{\text{g}}$ is the mass flow rate of the exhaust gas, $C_{\text{P,g}}$ is the specific heat capacity at constant pressure of the exhaust gas, and the term $(T_2 + \Delta T_{\text{amb}})$ represents the minimum possible value of the exhaust gas temperature at the outlet of the HRU which can be achieved for a given application.

Net power output

$$W_{\text{n}} = W_{\text{exp,actual}} - W_{\text{p,actual}}, \tag{26}$$

where W_{n} is the rate of net power output, $W_{\text{expactual}}$ is the rate of actual work done by expander and W_{pactual} is the rate of actual work done by pump.

Thermal efficiency of ORC

It indicates the ratio of useful work derived from the quantity of heat available in the heat source:

$$\eta_{\text{th}} = \frac{W_{\text{n}}}{Q_{\text{source}}} = \frac{W_{\text{exp,actual}} - W_{\text{p,actual}}}{Q_{\text{source}}}, \tag{27}$$

where Q_{source} is the heat sources from turbine exhaust.

Back work ratio (BWR)

It is the ratio of pump consumption to turbine output power.

$$\text{BWR} = \frac{W_{\text{p,actual}}}{W_{\text{T,actual}}}. \tag{28}$$

Efficiency enhancement

The efficiency enhancement of the combine cycle plant represents the total efficiency of the combined cycle relative to the efficiency of gas turbine power plant, expressed as

$$\eta_{GT+ORC} = \frac{W_{GT} + W_{ORC}}{\dot{m}_F \times LHV}. \quad (29)$$

Selection of working fluids for ORC system

Based on careful consideration of factors such as temperature range of the working fluid (between 520 and 300 °C for the heat source and 90 °C for the heat sink), critical temperature, environmental compatibility, cost, availability, and the thermo-physical properties as well as recommendations from similar studies (Fakeye and Oyedepo, 2018), five screened organic working fluids selected are: R245fa, R141b, R123, toluene and ethanol. The properties of the selected working fluids are highlighted in Table 4.

Results and discussion

This section discusses the results obtained from the thermodynamic analyses of the adapted basic ORC configuration developed to maximize the network output of the waste heat-to-power conversion of the exhaust gas of the selected gas turbine power plant. Based on the results, performance comparisons are made for the different operation regimes to determine the best power output at the different operation regimes and the most suitable working fluid that provides the optimal performance at the different operation regimes.

Performances at full and partial electric generator loads (EGLs)

Figure 4 compares the net power outputs per unit mass of the five selected working fluids at full load and partial loads (i.e., 100%; 75% and 50%) operating conditions of the electric generator. Figure 5 presents the mass flow rate that delivers the maximum power for the working fluids. For the range of electric generator load of 50–100%, the net power output varies as follows; R123 (220.83–405.28 kW); R141b (219.01–401.96 kW); R245fa (280.1–469.09 kW); Ethanol (109.76–199.31 kW) and Toluene (290.25–532.70 kW). At the same range of EGL, the mass flow rate of the selected working fluids that delivered the net power outputs varies as follows R123 (10.91–20.02 kg/s); R141b (9.50–17.43 kg/s); R245 fa (13.62–23.58 kg/s); ethanol (9.93–18.22 kg/s) and toluene (9.88–17.95 kg/s). The thermodynamic framework shows toluene to deliver the highest net power outputs at two operating regimes (at full load and 75% EGL) with capacity to generate 1.1063 MW of electricity from the exhaust fumes of the gas turbine when operating at full load and 0.66058 MW at partial electric generator loads of 75%. The performance of Toluene is closely followed by R245fa which delivers 0.955596 MW, 0.57447 MW and 0.28685 MW at 100% EGL, 75% EGL and 50% EGL, respectively.

From Figs. 4 and 5, Toluene has the best net power output per unit mass and comparatively the best mass flow rates. The mass flow rate has significant effect on the sizing and

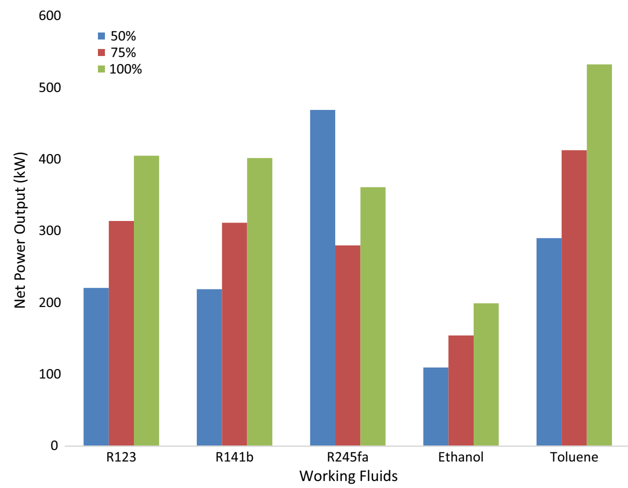

Fig. 4 Comparison of peak power output at full and partial EGLs

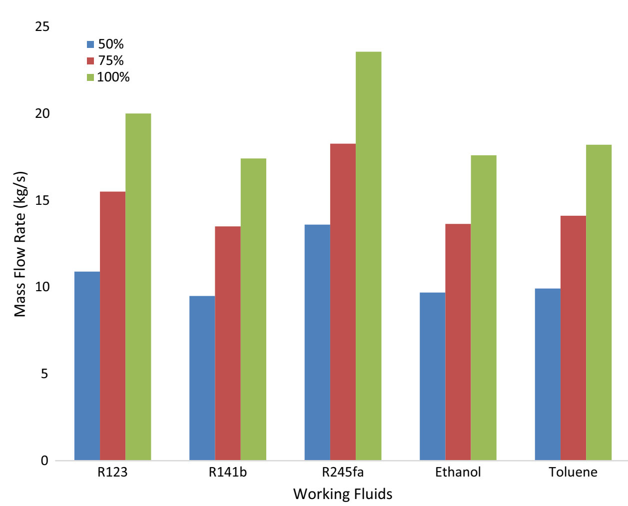

Fig. 5 Comparison of mass flow rate of working fluids at peak power output

Table 4 Properties of pre-selected working fluids

Working fluid	Type of fluid	Critical pressure (bar)	Critical temperature (°C)	Latent heat (kJ/kg)
R123	Dry	36.68	183.68	170.6
R141b	Isentropic	42.12	204.35	223
R245fa	Dry	36.51	154	196
Ethanol	Wet	62.68	241.56	864
Toluene	Dry	41.26	318.64	358

hence, on the cost of the ORC components. Lower mass flow rates imply smaller components. Hence, toluene shows overall best performances among the fluids examined within the constraints specified for all the operation regimes with respect to power output and mass flow rate criteria. This is in agreement with Cao et al. (Cao et al. 2016) that Toluene is the most preferred for GT-ORC combined cycles and also consistent with the recommendation of Carcasci et al. (2014) proposing toluene for WHR application operating between condenser temperature 27–87 °C and evaporation temperature of above 200 °C. Ethanol has the least net power output. R245fa, however, shows best adaptability at 50% electric generator load condition but nonetheless, disadvantaged with the highest mass flow rate, as depicted in Fig. 5. From Fig. 6a–c, toluene shows insignificant variation in net power output with respect to degree of superheat (DSH) and hence does not require a superheater. Noting that the efficiency enhancement of the combine cycle plant denotes the overall efficiency of the combined cycle relative to the efficiency of gas turbine power plant as expressed by Eq. (29), depending on the working fluid and superheating, efficiency enhancement obtained ranged from 51.46 to 54.19% using toluene and R245fa. However, toluene having the highest critical properties and specific enthalpy drop during expansion, it is possible that the power generated at slightly higher evaporator temperatures, and consequently, evaporator pressure above 30 bar may be superior to all other fluids without the need of superheating for being a dry fluid. Ethanol, being a wet fluid showed the poorest performance in the net power output with excessively large mass flow rates.

In some thermodynamic cycles with wet fluid, super heating is essential to keep the expansion in vapor phase and to prevent wet expansion and erosion in turbine. Since most ORCs use dry fluids, having excessive superheating is proven to have negative effect on maximum working pressure, saturation temperature and performance of the cycle (Bamgbopa, 2012). Figure 6a–c shows the variation of the net power output (kW) with the degree of superheating at full and partial loads for the five selected working fluids within the optimal range of 40 °C of superheating. For all the working fluids considered, as the load increases from 50 to 100%, the net power output also increases except for R123. As expected, Toluene and R245fa (dry fluids) in Fig. 6a show mild improvement in net power delivered as well as efficiency with increase in superheating (Zhou et al. 2013; Lion and Lion, 2017; Liu et al. 2012). Ethanol (wet fluid) also shows mild improvement with increase in superheating, while the only R141b (isentropic fluid) shows no appreciable response to the degree of superheating. This, however, is consistent with literature (Jung et al. 2014).

However, results show a general decrease in mass flow rate as the degree of superheating increases for all the working fluids. Figure 7a–c shows the variation of mass flow

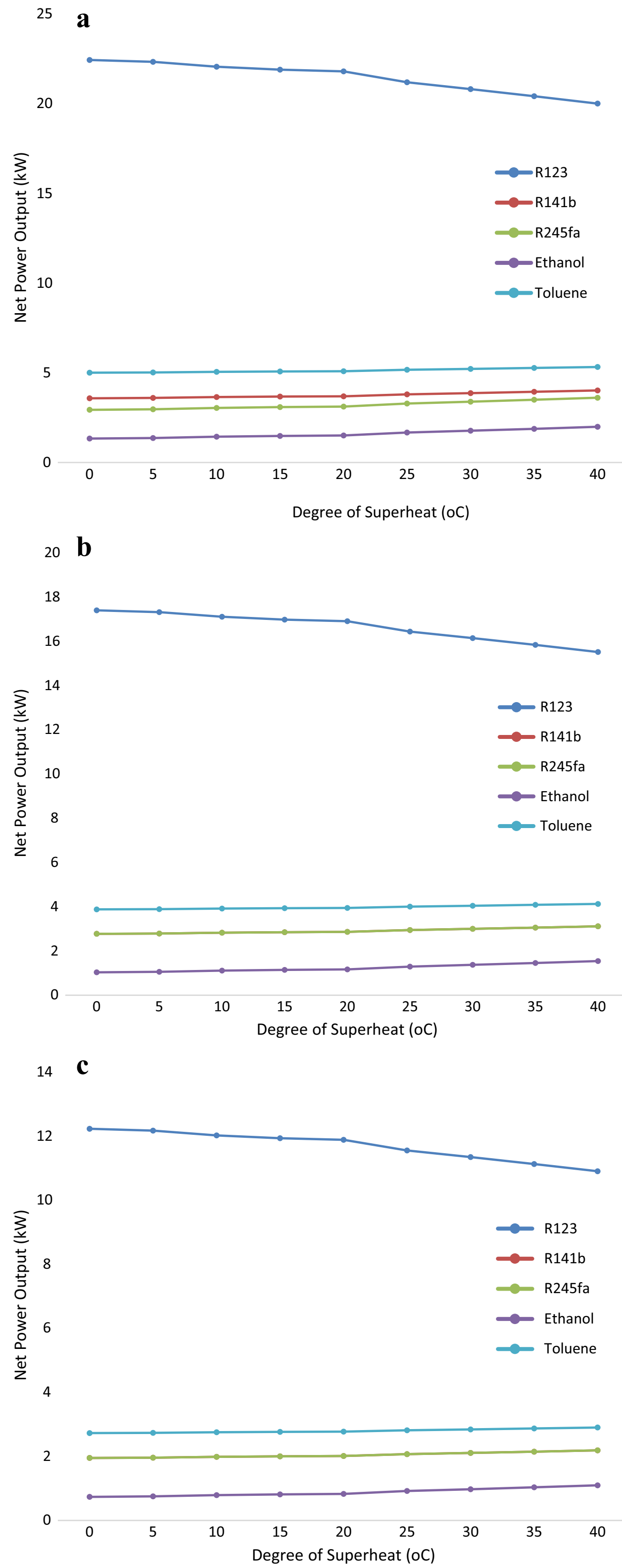

Fig. 6 **a** Variation of net power output with DSH at full load. **b** Variation of net power output with DSH at 75% EG load. **c** Variation of net power output with DSH at 50% EG load

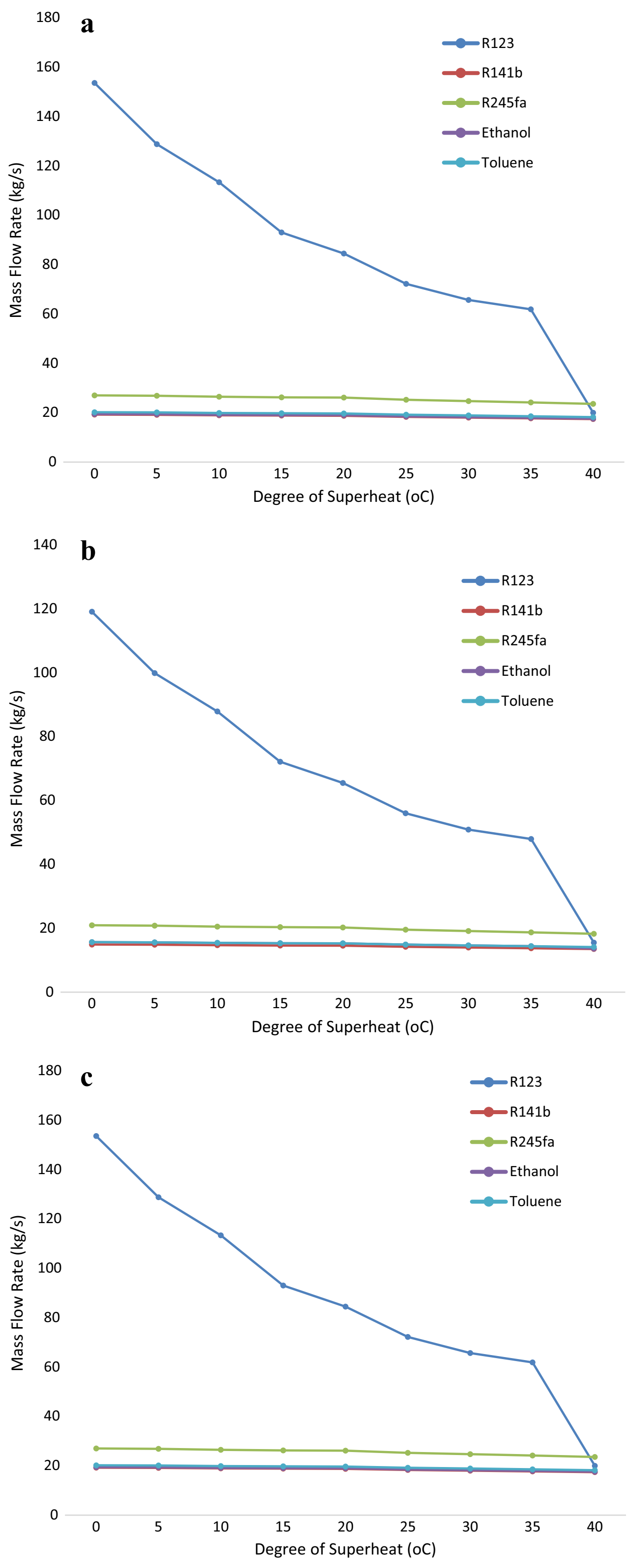

Fig. 7 **a** Variation of mass flow rate with degree of superheat at full load. **b** Variation of mass flow rate with degree of superheat at 75% EG Load. **c** Variation of mass flow rate with degree of superheat at 50% EG load

rate with the degree of superheating at the various regimes considered. R123 shows the highest response to variation in mass flow rate with the degree of superheating, followed by R245fa, while R141b show insignificant response which is a situation generally suitable for superheating of isentropic fluids. At 35 °C of superheat, all the working fluids show decrease in mass flow rate.

Conclusion

In this study, five different candidates of organic working fluids for assessment of waste heat recovery from a 5.76 MW gas turbine power plant using ORC system were evaluated. The net power output and mass flow rate of these working fluids have been investigated at different electric generator loads of 50%, 75% and 100%. Thermodynamic model of the ORC system was analysed and simulated using MATLAB codes developed by the authors and the thermodynamic data at each state of the ORC system were supplied by engineering equation solver (EES). The thermodynamic models developed in this work constitute a generic formulation that can be integrated into a global optimization routine for the preliminary design analysis of waste heat recovery systems, essentially to optimize the mass flow rate that maximizes the net power output to obtain cost effective and compact equipment sizes.

The implementation of the thermodynamic framework shows Toluene to be the most suitable working fluid for the three operating regimes with capacity to generate 532.70 kW of electricity from the exhaust fumes of the gas turbine when operating at full load and 412.95 kW and 290.25 kW when operating at partial electric generator loads of 75% and 50%, respectively. These values were achieved at the least mass flow rates and this increased the overall efficiency of the combined cycle system by 16.85% at full load and 10.1% at 50%EGL. R123 also exhibited good performance next to Toluene with peak net power output of 405.28 kW at full load, 314.18 kW and 220.83 kW at 75% and 50% EG loads, respectively.

R245fa exhibited highest net power output of 469.09 kW at 50% partial load but with excessively high mass flow rates where is shows good adaptability. From the study, ethanol showed the least performance but being a wet fluid, would require piston or scroll expander to handle two-phase expansion (Oyedepo and Fakeye 2019).

Acknowledgements The authors acknowledge Covenant University Management for the research support received from CUCRID, Covenant University, Ota.

References

Abadi, Bamorovat, and Kim, K. C. (2017). Investigation of organic Rankine cycles with zeotropic mixtures as a working fluid: advantages and issues. *Renewable and Sustainable Energy Reviews, 73,* 1000–1013.

Auld, A., Berson, A., and Hogg, S. (2013). Organic rankine cycles in waste heat recovery: a comparative study. *International Journal of Low-Carbon Technologies, 8*(SUPPL1), 9–18. https://doi.org/10.1093/ijlct/ctt033.

Badescu, V., Aboaltabooq, M. H. K., Pop, H., Apostol, V., Prisecaru, M., and Prisecaru, T. (2017). Design and operational procedures for ORC-based systems coupled with internal combustion engines driving electrical generators at full and partial load. *Energy Conversion and Management, 139,* 206–221. https://doi.org/10.1016/j.enconman.2017.02.046.

Bamgbopa, M. O. (2012). Modeling and performance evaluation of an organic Rankine cycle (Orc) with R245Fa as working fluid. M.Sc Thesis, Middle East Technical University, Northern Cyprus Campus, pp 1–80.

Bao, J., and Zhao, L. (2013). A review of working fluid and expander selections for organic Rankine cycle. *Renewable and Sustainable Energy Reviews, 24,* 325–342. https://doi.org/10.1016/j.rser.2013.03.040.

Cao, Y., Gao, Y., Zheng, Y., and Dai, Y. (2016). Optimum design and thermodynamic analysis of a gas turbine and ORC combined cycle with recuperators. *Energy Conversion and Management, 116,* 32–41. https://doi.org/10.1016/j.enconman.2016.02.073.

Carcasci, C., Ferraro, R., and Miliotti, E. (2014). Thermodynamic analysis of an organic Rankine cycle for waste heat recovery from gas turbines. *Energy, 65,* 91–100. https://doi.org/10.1016/j.energy.2013.11.080.

Chen, Y. (2011). Thermodynamic cycles using carbon dioxide as working fluid—CO2 transcritical power cycle study, PhD Thesis.

Donghong, W., Xuesheng, L., Zhen, L., and Jianming, G. (2007). Performance analysis and optimization of organic Rankine cycle (ORC) for waste heat recovery. *Energy Conversion and Management, 48,* 1113–1119.

Dubberke, et al. (2018). Experimental setup of a cascaded two-stage organic Rankine cycle. *Applied Thermal Engineering, 131,* 958–964.

Eveloy, V., Rodgers, P., Olufade, A., Wang, Y., and Alili, A. A. (2016). Waste heat recovery from gas turbine flue gases for power generation enhancement in a process plant. *The International Journal of Thermal and Environmental Engineering, 12*(1), 53–60. https://doi.org/10.5383/ijtee.12.01.007.

Fakeye, B. A., and Oyedepo, S. O. (2018). A review of working fluids for organic Rankine cycle (ORC) applications. *IOP Conference Series Materials Science and Engineering*. https://doi.org/10.1088/1757-899x/413/1/012019.

Feng, Y., Hung, T. C., Zhang, Y., Li, B., Yang, J., and Shi, Y. (2015). Performance comparison of low-grade ORCs (organic Rankine cycles) using R245fa, pentane and their mixtures based on the thermoeconomic multi-objective optimization and decision makings. *Energy, 93*(2015), 2018–2029. https://doi.org/10.1016/j.energy.2015.10.065.

Guo, C., Du, X., Yang, L., and Yang, Y. (2015). Organic Rankine cycle for power recovery of exhaust flue gas. *Applied Thermal Engineering, 2015*(75), 135–144. https://doi.org/10.1016/j.applthermaleng.2014.09.080.

Hattiangadi, A. (2013). Working fluid design for organic Rankine cycle (ORC) systems. M.Sc Thesis, Faculty of Applied Sciences, Delft University of Technology, pp 1–99. http://repository.tudelft.nl/assets/uuid:492ce6c0-ab22-42d0-ba00-3cf3702eb873/MSc_SET_Akshay_Hattiangadi_Final_Thesis.pdf. Accessed 3 June 2019.

Jung, H. C., Krumdieck, S., and Vranjes, T. (2014). Feasibility assessment of refinery waste heat-to-power conversion using an organic Rankine cycle. *Energy Conversion and Management, 77,* 396–407.

Kai, Z., Mi, Z., Yabo, W., Zhili, S., Shengchun, L., and Jinghong, N. (2015). Parametric optimization of low temperature ORC system. *Energy Procedia, 75,* 1596–1602. https://doi.org/10.1016/j.egypro.2015.07.374.

Landelle, A., Tauveron, N., Revellin, R., Haberschill, P., and Colasson, S. (2017). Experimental Investigation of a transcritical organic Rankine cycle with scroll expander for low-temperature waste heat recovery. *Energy Procedia, 129,* 810–817. https://doi.org/10.1016/j.egypro.2017.09.142.

Lecompte, S., Huisseune, H., Van Den Broek, M., Vanslambrouck, B., and De Paepe, M. (2015). Review of organic Rankine cycle (ORC) architectures for waste heat recovery. *Renewable and Sustainable Energy Reviews, 47,* 448–461. https://doi.org/10.1016/j.rser.2015.03.089.

Li, P., Han, Z., Jia, X., Mei, Z., Han, X., and Wang, Z. (2019). Comparative analysis of an organic Rankine cycle with different turbine efficiency models based on multi-objective optimization. *Energy Conversion and Management, 185,* 130–142.

Li, Y. R., Wang, J. N., and Du, M. T. (2012). Influence of coupled pinch point temperature difference and evaporation temperature on performance of organic Rankine cycle. *Energy, 42*(1), 503–509. https://doi.org/10.1016/j.energy.2012.03.018.

Lion, S., and Lion, S. (2017). A thermodynamic feasibility study of an organic Rankine cycle (ORC) for heavy-duty diesel engine waste heat recovery in off-highway applications. *International Journal of Energy and Environmental Engineering*. https://doi.org/10.1007/s40095-017-0234-8.

Liu, C., He, C., Gao, H., Xu, X., and Xu, J. (2012). The optimal evaporation temperature of subcritical ORC based on second law efficiency for waste heat recovery. *Entropy*. https://doi.org/10.3390/e14030491.

Oyedepo S. O., and Fakeye B. A. (2019). Designing optimized organic Rankine cycles systems for waste heat-to-power conversion of gas turbine flue gases. *Journal of Physics: Conference Series, 1378,* 032097. https://doi.org/10.1088/1742-6596/1378/3/032097

Pierobon, L., Nguyen, T.-V., Larsen, U., Haglind, F., and Elmegaard, B. (2013). Multi-objective optimization of organic Rankine cycles for waste heat recovery: Application in an offshore platform. *Energy, 58,* 538–549. https://doi.org/10.1016/j.energy.2013.05.039.

Quoilin, S., Aumann, A., Grill, A., Schuster, A., Lemort, V., and Spliethoff, H. (2011). Dynamic modeling and optimal control strategy of waste heat recovery organic Rankine cycles. *Applied Energy, 88*(6), 2183–2190.

Reis, M. M. L., and Gallo, W. L. R. (2018). Study of waste heat recovery potential and optimization of the power production by an organic Rankine cycle in an FPSO unit. *Energy Conversion and Management, 157,* 409–422. https://doi.org/10.1016/j.enconman.2017.12.015.

Roberto, A., and Lars, O. N. (2017). Fluid selection and thermodynamic optimization of organic Rankine cycles for waste heat recovery applications. *Energy Procedia, 129,* 527–534.

Rusev, T. M. (2014). Comparative study of different organic Rankine cycle models: simulations and thermo-economic analysis for a gas engine waste heat recovery application. M.Sc Thesis, KTH School of Industrial Engineering and Management, Stockholm, pp. 1–77.

Safarian, S., and Aramoun, F. (2015). Energy and exergy assessments of modified organic Rankine cycles (ORCs). *Energy Reports, 1,* 1–7. https://doi.org/10.1016/j.egyr.2014.10.003.

Sung, T., Yun, E., Kim, H. D., Yoon, S. Y., Choi, B. S., Kim, K., et al. (2016). Performance characteristics of a 200-kW organic Rankine cycle system in a steel processing plant. *Applied Energy, 183,* 623–635. https://doi.org/10.1016/j.apenergy.2016.09.018.

Tailu, L., Qiulin, W., Jialing, Z., Kaiyong, H., and Wencheng, F. (2015). Thermodynamic optimization of organic Rankine cycle using two stage evaporation. *Renewable Energy, 75,* 654–664. https://doi.org/10.1016/j.renene.2014.10.058.

Wang, H., Xu, J., Yang, X., Miao, Z., and Yu, C. (2015). Organic Rankine cycle saves energy and reduces gas emissions for cement production. *Energy, 86,* 59–73. https://doi.org/10.1016/j.energy.2015.03.112.

Wenqiang, S., Xiaoyu, Y., and Yanhui, W. (2017). Exergy efficiency analysis of ORC (organic Rankine cycle) and ORC based combined cycles driven by low-temperature waste heat. *Energy Conversion and Management, 135,* 63–73.

Xi, X., Zhou, Y., Guo, C., Yang, L., and Du, X. (2015). Characteristics of organic Rankine cycles with zeotropic mixture for heat recovery of exhaust gas of boiler. *Energy Prcedia, 75,* 1093–1101. https://doi.org/10.1016/j.egypro.2015.07.496.

Xiao, L., Shuang-Ying, W., Tian-Tian, Y., Chao, L., and You-Rong, L. (2015). Multi-objective optimization of evaporation and condensation temperatures for subcritical organic Rankine cycle. *Energy, 83,* 723–733.

Xiaojun, Z., Lijun, W., Xiaoliu, W., and Guidong, J. (2016). Comparative study of waste heat steam SRC, ORC and S-ORC power generation systems in medium-low temperature. *Applied Thermal Engineering, 106,* 1427–1439.

Yu, H., Feng, X., Wang, Y., Biegler, L. T., and Eason, J. (2016). A systematic method to customize an efficient organic Rankine cycle (ORC) to recover waste heat in refineries. *Applied Energy, 179,* 302–315. https://doi.org/10.1016/j.apenergy.2016.06.093.

Zhou, N., Wang, X., Chen, Z., and Wang, Z. (2013). Experimental study on organic Rankine cycle for waste heat recovery from low-temperature flue gas. *Energy, 55,* 216–225. https://doi.org/10.1016/j.energy.2013.03.047.